Research Article

Journal of Environmental Nanotechnology

Carbon Dioxide Decomposition over $AlPO_4$-based Molecular Sieves

S. Siva Sankari, M.A. Mary Thangam, Chellapandian Kannan*
Department of Chemistry, Manonmaniam Sundaranar University, Tirunelveli, TN, India
Received: 08.11.2018 Accepted: 25.12.2018 Published: 30-03-2019
*chellapandiankannan@gmail.com

ABSTRACT

Carbon dioxide is the most prevalent greenhouse gas that traps heat and raises the global temperature. To minimize this undesirable climate change, solid acid catalysts are to be used for the decomposition of CO_2. Aluminophosphate molecular sieves have wide applications in the field of catalysis and adsorption. In this work, metal-incorporated aluminophosphate molecular sieves *viz*, magnesium aluminophosphate and manganese aluminophosphate (Mg-$AlPO_4$ and Mn-$AlPO_4$) were synthesized using low-cost n-butyl amine as a new template for high activity in the decomposition of CO_2 into CO and O_2. The FT-IR spectrum confirmed the formation of the tetrahedral framework of the materials. Powder X-ray diffraction pattern of calcinated Mg-$AlPO_4$ and Mn-$AlPO_4$ proved the well-crystalline nature of the material. The morphology of the material was studied by using SEM analysis. The BET surface area of calcinated Mg-$AlPO_4$ and Mn-$AlPO_4$ confirmed the nanoporous nature of the materials. Carbon dioxide was decomposed in a catalytic reactor using Mg-AlPO4 and Mn-AlPO4 as catalysts. For maximal CO_2 conversion, the catalytic reaction parameters such as temperature, flow rate, catalyst dose and time on stream were determined. The conversion and product selectivity were dependent upon the acidity and pore size of the catalysts.

Keywords: Carbon dioxide decomposition; n-butyl amine; Mg-$AlPO_4$; Mn-$AlPO_4$.

1. INTRODUCTION

Global warming is caused by increased emissions of greenhouse gases (mainly carbon dioxide) into the atmosphere. Generally, polymeric adsorbents, zeolites, silica gels, activated carbons and molecular sieves have been extensively used as selective adsorbents because of their controllable pore structures and surface properties, which can be used to selectively capture CO_2 (Anastas *et al*. 2001; Taguchi and Schuth, 2005). Among these adsorbents, molecular sieves have the ability to selectively absorb specific components of gaseous mixtures because of their porous structures, which consist of relatively uniform pores. The porous solid acid materials are green catalysts for organic reactions. Solid acids are generally categorized by their type - 'Brownsted acids' or 'Lewis acids' (Liu *et al.* 2006). They are based on micelle-template silica and other mesoporous high surface area support materials are beginning to play a significant role in the greening of fine and specialty chemical manufacturing processes (Ruthven, 1984). A solid acid catalyst has an advantage, such as easy operation for isolating a product after the reaction (Smit and Maesen, 2008). Heteroatom-containing aluminophosphate molecular sieves are of a prime class of heterogeneous single-site solid catalysts. Aluminophosphate plays an important role in the field of catalysis and adsorption (Pai *et al.* 2008). The application depends on its pore size, acidity, surface area and stability. In order to increase the catalytic activity of nanoporous $AlPO_4$ molecular sieves, the metal ions are incorporated into the framework of $AlPO_4$ (Gao *et al.* 1997). In this work, metal-incorporated aluminophosphate molecular sieves *viz*, magnesium aluminophosphate and manganese aluminophosphate (Mg-$AlPO_4$ and Mn-$AlPO_4$) were synthesized by Sol-gel method using n-butyl amine as a new template. The carbon dioxide decomposition reaction was used to investigate the catalytic activity of the catalysts. Temperature, flow rate, catalyst dosage and duration on stream were optimized in the lab to get the maximum CO_2 conversion. The regeneration of catalysts was performed by the thermal method in the presence of air.

2. EXPERIMENTAL METHODS

2.1 Materials

The chemicals for the synthesis of nanoporous aluminophosphate were aluminium hydroxide (Merck, GR), orthophosphoric acid (Nice, GR) and n-butyl amine (Loba Chemie, GR). The metal sulphates used for the isomorphous substitution in the $AlPO_4$ framework were magnesium sulphate and manganese sulphate (Merck, GR), respectively.

2.2 Characterization

The Fourier Transform Infrared (FT-IR) measurements of samples were recorded by JASCO-410 FT-IR model Spectrophotometer by using KBr pellet technique. X-ray diffraction patterns were recorded on a PANalytical X'Pert Pro Powder X'Celerator Diffractometer using Cu-Kα radiation (λ = 1.5406 Å) with a voltage of 40 kV and current of 30 mA. The SEM images were recorded by Carl Zeiss Evo 18 Scanning Electron Microscope with the voltage 20 kV. The surface areas of the samples were obtained by Brunauer-Emmett Teller (BET) method and the pore size distribution was calculated from the BJH method. Nitrogen adsorption-desorption measurements were made using Smart Instruments Co. Pvt. Ltd., Smart Sorb 92/93; the samples were outgassed at 200 ˚C for one h.

2.3 Synthesis of Metal Ion-substituted Aluminophosphate Molecular Sieves

Aluminium hydroxide and orthophosphoric acid were chosen as the source material for aluminium and phosphorous, respectively. 9.8 ml of n-butylamine was dissolved in 150 ml of de-ionized water. Then 7.8 g of aluminium hydroxide was added in 100 ml of water and added slowly into the template solution and stirred for one hour. About 9.8 g (5.2 ml) of orthophosphoric acid was dissolved in 50 ml of water and isomorphous substitution of metal ions was taking place by adding 0.02 mole of magnesium sulphate (2.406 g) or manganese sulphate (3.02 g) into the above mixture and stirred continuously for 2 h to attain a homogeneous mixture. The resulting mixture was dried in a hot air oven at 120 ˚C and washed thoroughly with de-ionized water until the pH of the discarded solution became neutral. The solid was then filtered and dried at 120 ˚C in a hot air oven. The gel compositions were 0.98 Al_2O_3:P_2O_5:n-A:0.02 MgO:300 H_2O and 0.98 Al_2O_3:P_2O_5:n-BA:0.02 MnO:300 H_2O. The synthesized material was calcinated at 400 ˚C for 4 h to remove the organic template present in the pores of the molecular sieves.

2.4 Catalytic Reactor

The catalytic activity studies were carried out in the gas phase. The required amount of calcinated catalysts was taken in a U-shaped tube. One end of the tube was connected to a carbon dioxide cylinder and the other end was connected to the bottle containing silica gel to absorb moisture, as shown in Fig. 1.

The carbon dioxide was flowing into the catalyst and the decomposition of CO_2 was taking place to produce different products. The reaction products were taken from the outlet tube using a syringe and the products were analyzed by gas chromatography.

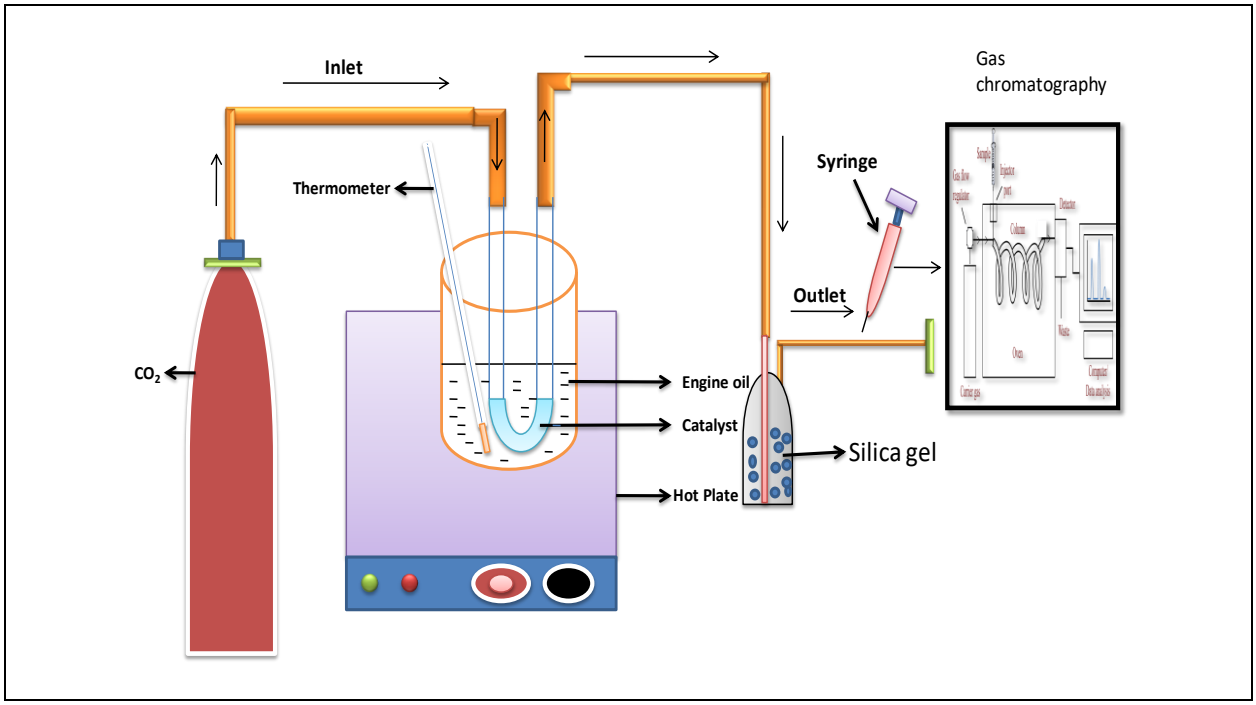

Fig. 1: Catalytic reactor for the decomposition of CO_2

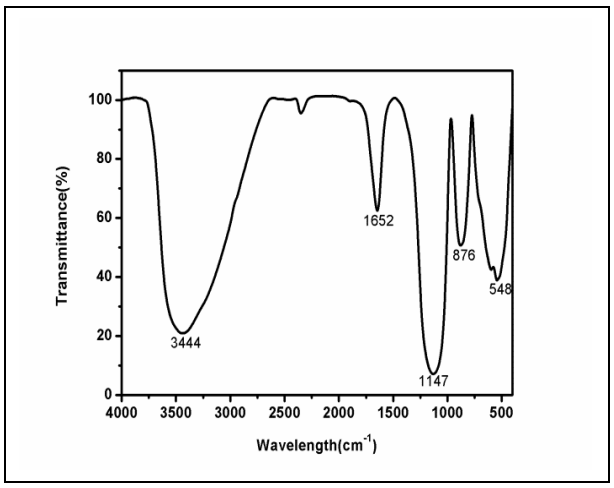

Fig. 2 (a): FT-IR spectrum of synthesized Mg-AlPO$_4$

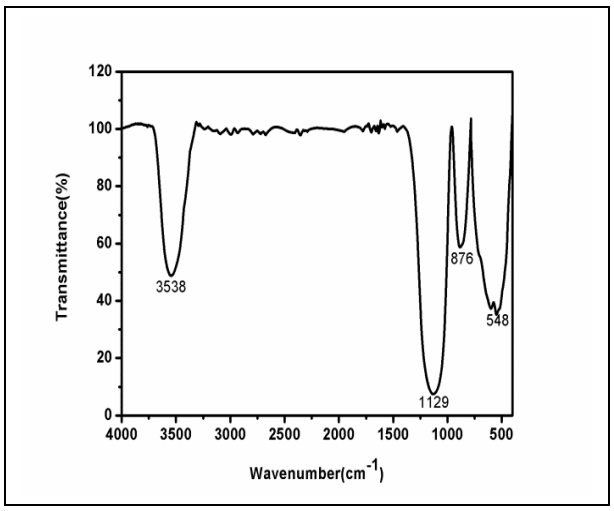

Fig. 2 (b): FT-IR spectrum of calcinated Mg-AlPO$_4$

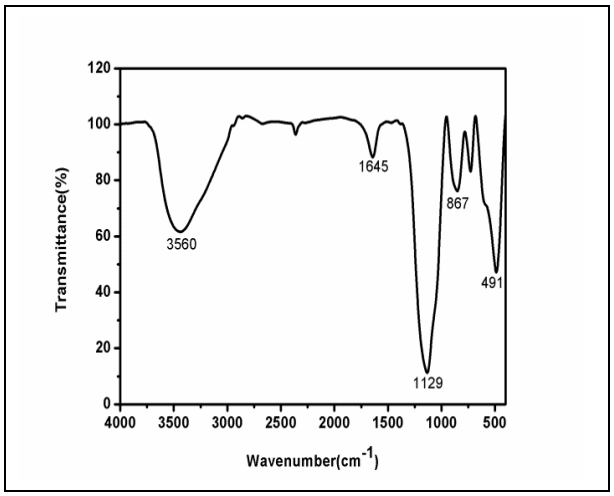

Fig. 3 (a): FT-IR spectrum of synthesized Mn-AlPO$_4$

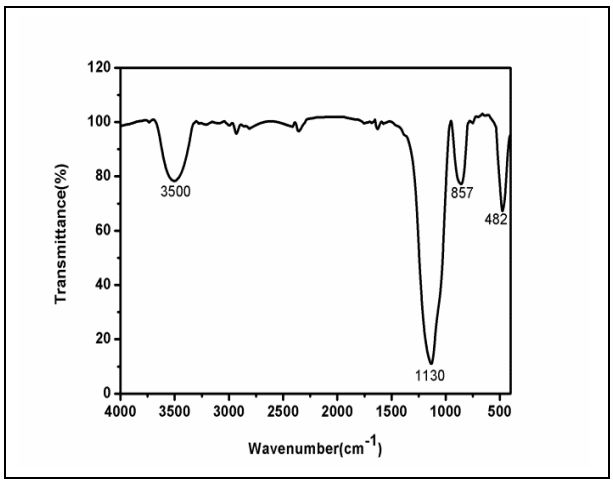

Fig. 3 (b): FT-IR spectrum of calcinated Mn-AlPO$_4$

3. RESULTS AND DISCUSSION

3.1 FT-IR Spectrum

Fig. 2 (a) and 3 (a) have revealed the strong broadband at 3400-3600 cm^{-1}, which was assigned to the O-H vibration of water molecule present in the as-synthesized sample, whereas in calcinated samples (Fig. 2 (b) and 3 (b)), the –OH bond became weak. The asymmetric stretching vibrations of tetrahedral aluminophosphate were observed near 1100 cm^{-1} (Campelo *et al.* 2003). The symmetric stretching and bending mode were observed near 700 and 500 cm^{-1} (Campelo *et al.* 1986).

The C-H deformation band, C-N band and N-H bending band at 1460 cm^{-1}, 1350 cm^{-1} and 1500 cm^{-1} were present in the as-synthesized sample whereas in calcinated sample these bands were absent. This proved that there was a complete removal of template molecule from the as-synthesized sample after calcination. The peaks between 1000 cm^{-1} and 1200 cm^{-1} have confirmed the presence of metal ions in the tetrahedral framework (Cheralathan *et al.* 2000).

3.2 Powder X-ray Diffraction Analysis

The powder X-ray diffraction pattern of calcinated Mg-AlPO$_4$ and Mn-AlPO$_4$ are shown in Fig. 4 and Fig. 5 respectively, which revealed the well-crystalline nature of the material (Tanev and Pinnavaia, 1995). The d–spacing values of the materials were closely matched with the JCPDS files (881680 and 511755) and it has been confirmed that the materials were in hexagonal structure (Table 1). The average crystal sizes of Mg-AlPO$_4$ and Mn-AlPO$_4$ were 7.60 nm and 18.91 nm, respectively.

Table 1. XRD parameters for Mg-$AlPO_4$ and Mn-$AlPO_4$

Catalyst	Lattice	System	h	k	l	2 θ	d-spacing (Å)	
							Standard	Observed
Mg-$AlPO_4$	Primitive	Hexagonal	6	2	2	45.9433	1.9722	1.97537
			0	0	6	67.0747	1.3944	1.39541
Mn-$AlPO_4$	Primitive	Hexagonal	2	1	0	20.3601	4.3294	4.36193
			2	1	1	21.5084	4.1139	4.13158
			0	0	7	45.5887	1.9057	1.98990
			3	2	8	66.7122	1.4071	1.40211

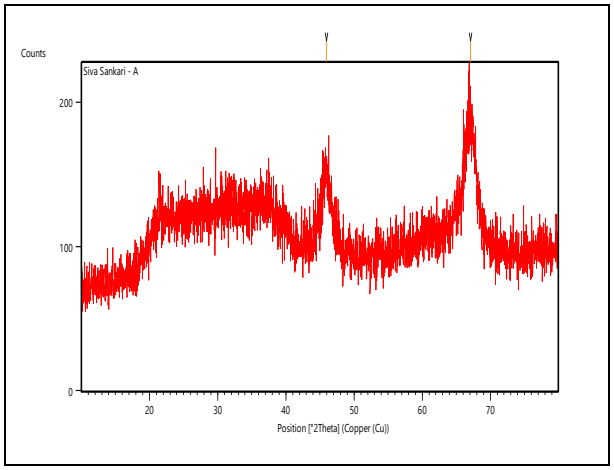

Fig. 4: XRD pattern of calcinated Mg-$AlPO_4$

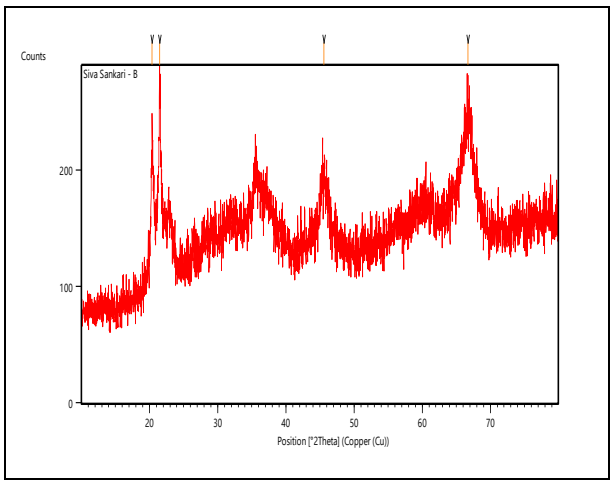

Fig. 5: XRD pattern of calcinated Mn-$AlPO_4$

3.3 Scanning Electron Microscopic Analysis

Fig. 6 and 7 show the SEM images of calcinated Mg-AlPO4 and Mn-AlPO4, respectively. The crystalline nature of the metal ion-inserted $AlPO_4$ materials was depicted by the SEM images. The variation in morphology and pore creation among the Mg-$AlPO_4$ and Mn-$AlPO_4$ was evidence for the metal ion-incorporation in the tetrahedral framework of the molecular sieves (Hardie *et al.* 2005).

3.4 Surface Area and Pore Size Distribution

The BET surface areas of calcinated Mg-$AlPO_4$ and Mn-$AlPO_4$ were 71.66 m^2/g and 49.39 m^2/g; their pore diameters were 10 nm and 12 nm, respectively, thus confirming the nanoporous nature of the materials.

4. CATALYTIC APPLICATION

4.1 Decomposition of Carbon Dioxide over Nanoporous $AlPO_4$-based Molecular Sieves

The decomposition of carbon dioxide has been carried out over metal ion-incorporated catalysts *viz*, Mg-$AlPO_4$ and Mn-$AlPO_4$ under controlled experimental conditions; carbon dioxide was decomposed into carbon monoxide and oxygen. The optimum experimental conditions such as temperature, flow rate, catalyst dosage and time on stream were determined to find out the maximum conversion of CO_2 and product selectivity.

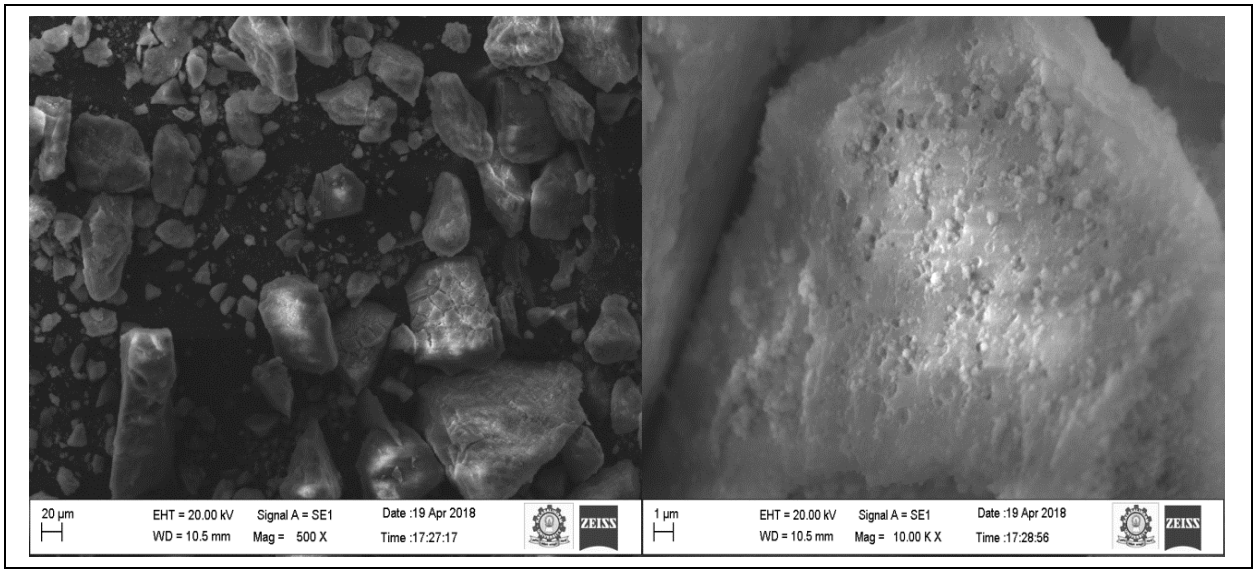

Fig. 6: SEM images of Mg-AlPO$_4$

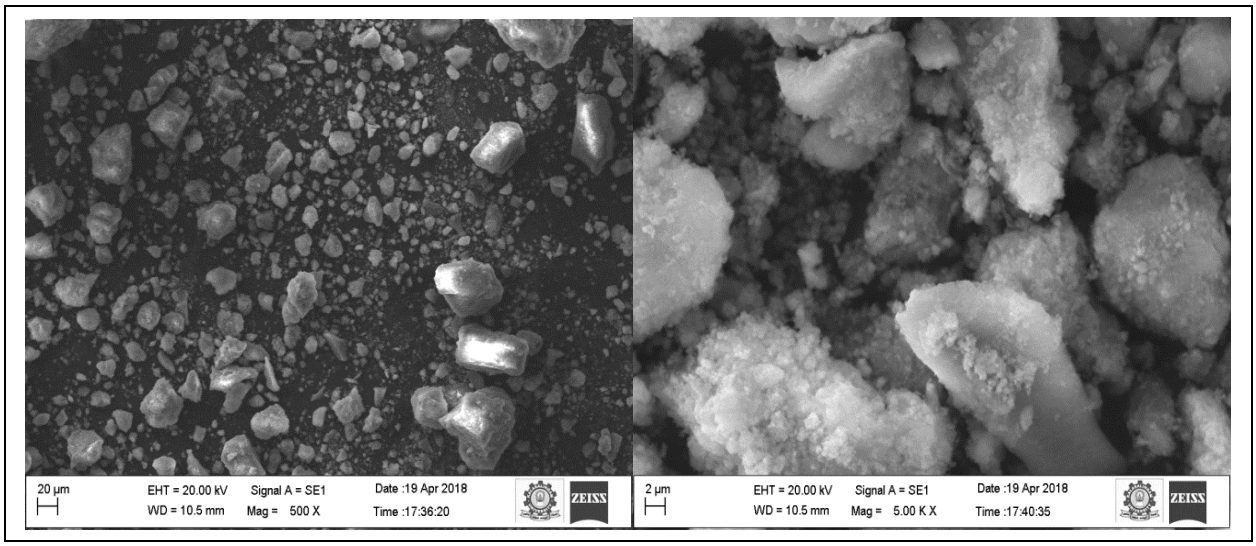

Fig. 7: SEM images of Mn-AlPO$_4$

4.1.1 Effect of Temperature

The influence of temperature on the decomposition of CO_2 has been studied on 0.5 g of Mg-AlPO$_4$ and Mn-AlPO$_4$ catalysts at the temperatures of 60, 70, 80, 150 and 200 $^{\circ}$C (Fig. 8). The percentage of conversion of carbon dioxide and the product selectivity with respect to temperature were shown in Table 2. In the case of Mg-AlPO$_4$, the maximum conversion was observed at 60 °C; no significant conversion has been found for further increase in temperature. This proved the high catalytic activity of the catalyst. In Mn-AlPO$_4$, the maximum conversion of carbon dioxide was found at 60 $^{\circ}$C and for further increase in temperature the conversion decreased. This proved that the catalytic activity of Mn-AlPO$_4$ decrease with the increase of temperature. The selectivity of oxygen decreases with the decrease in conversion, but carbon monoxide selectivity increases with the decrease in conversion. This may be due to the adsorption of oxygen inside the pores of the catalysts. This behaviour depends on the nature of the catalyst.

Table 2. Effect of Temperature over $MAlPO_4$

Catalyst	Temperature (ºC)	Conversion (%)	Product selectivity (%)	
			CO	O_2
Mg-$AlPO_4$	60	99.7986	44.5147	55.4855
	70	99.6991	48.9603	51.9027
	80	99.5456	50.7007	49.2994
	150	99.5356	51.1699	48.8301
	200	99.3237	48.0975	51.9027
Mn-$AlPO_4$	60	74.0109	52.3016	47.6983
	70	36.5067	76.2409	23.6466
	80	32.3018	94.7786	5.2214
	150	25.9584	93.0443	6.9557
	200	26.4061	91.8759	8.1243

Time: 1 h, Catalyst amount: 0.5 g, Flow rate: 0.5 ml/min

Table 3. Effect of Flow rate over $MAlPO_4$

Catalyst	Flow rate (ml/min)	Conversion (%)	Product selectivity (%)	
			CO	O_2
Mg-$AlPO_4$	0.5	99.3237	44.5147	55.4855
	1.5	15.0212	88.7905	11.2088
	2.5	12.8044	92.6415	7.3574
Mn-$AlPO_4$	0.5	74.0109	52.3016	47.6983
	1.5	11.0298	81.7825	18.2179
	2.5	13.3026	88.0046	11.9962

Time: 1 h, Catalyst amount: 0.5 g, Temperature: 60 ˚C

4.1.2 Effect of Flow rate

The effect of flow rate on the decomposition of carbon dioxide over 0.5 g of Mg-$AlPO_4$ and Mn-$AlPO_4$ catalysts has been studied from 0.5 to 2.5 ml per min (Fig. 9). The percentage of conversion and product selectivity with respect to flow rate were shown in Table 3. The maximum conversion of carbon dioxide was observed at 0.5 ml per min. With further increase in flow rate, the percentage of conversion decreased. The percentage of conversion increased with a decrease in CO_2 flow rate due to the longer residence time in the catalytic bed. The selectivity of oxygen decreased with the decrease in conversion, but carbon monoxide selectivity increased with conversion. This may be due to the adsorption of oxygen inside the pores of the catalysts. This behaviour depends on the nature of the catalyst.

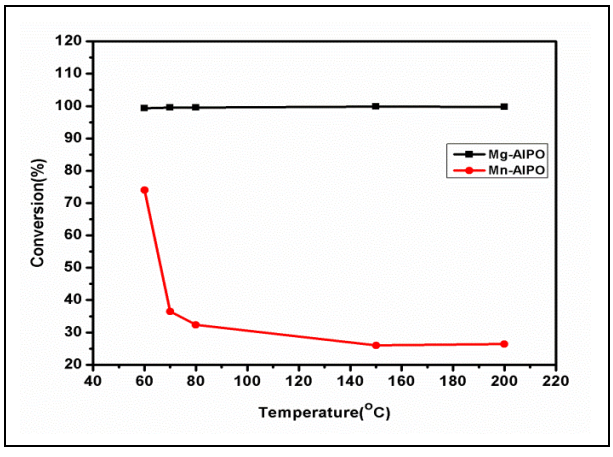

Fig. 8: Effect of Temperature on decomposition of CO_2 over $MAlPO_4$

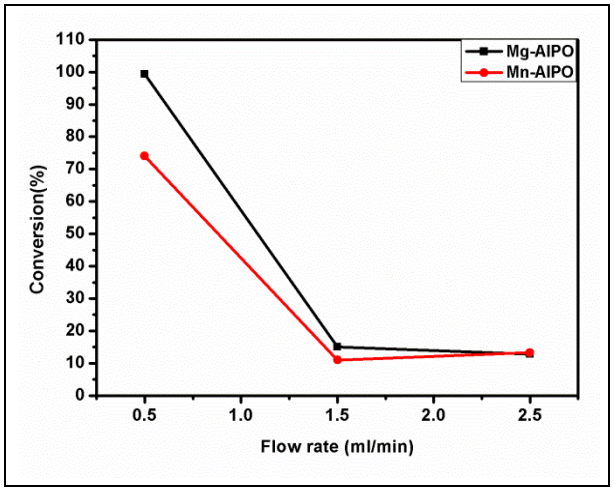

Fig. 9: Effect of Flow rate on the decomposition of CO_2 over $MAlPO_4$

4.1.3 Effect of Catalyst dosage

The effect of catalyst dosage on carbon dioxide decomposition reaction over Mg-$AlPO_4$ and Mn-$AlPO_4$ catalysts has been studied from 0.5 g to 1.5 g (Fig. 10). The percentage of conversion of carbon dioxide and selectivity of the products with respect to catalyst dosage were shown in Table 4. The maximum conversion was observed at 0.5 g; for further increase in catalyst dosage, the percentage of conversion decreased. At lower catalyst dosage, the conversion of CO_2 was occurring easily; at higher catalyst dosage, the re-combination of carbon monoxide and oxygen was taking place to form carbon dioxide in the catalytic bed due to the long pathway of the carbon monoxide and oxygen in the reactor. The selectivity of oxygen decreased with the decrease in conversion, but carbon monoxide selectivity increased with the decrease in conversion; this may be due to the adsorption of oxygen inside the pores of the catalysts. This behaviour depends on the nature of the catalyst.

4.1.4 Effect of Time on stream

From all the above experimental data, it was found that the maximum conversion of carbon dioxide was observed under the following experimental conditions:

Reaction temperature: 60 °C, Catalyst dosage: 0.5 g and Flow rate: 0.5 ml

The effect of time on stream has been studied over Mg-$AlPO_4$ and Mn-$AlPO_4$ up to 5 h (Table 5). The carbon dioxide decomposition decreased with the increase of time (Fig. 11). This may be due to the pressure of carbon dioxide in the reactor bed. The carbon dioxide flow was arrested at the outlet. Hence pressure was developed in the catalytic bed; hence, the carbon dioxide reaction reduces with increased flow rate. The selectivity of oxygen decreased with the decrease in conversion, but carbon monoxide selectivity increased with the decrease in conversion; this may be due to the adsorption of oxygen inside the pores of the catalysts. This behaviour depends on the nature of the catalyst.

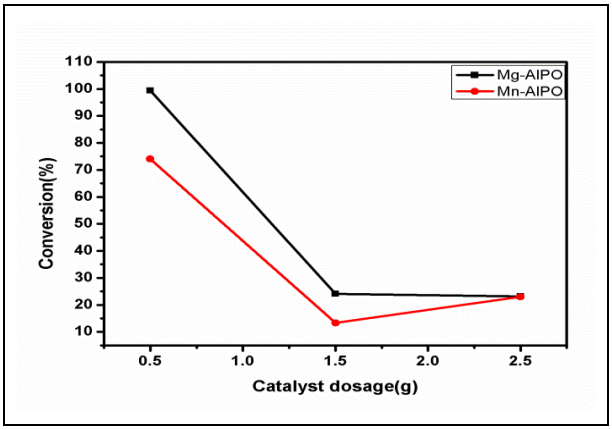

Fig. 10: Effect of catalyst dosage on the decomposition of CO_2 over $MAlPO_4$

Table 4. Effect of Catalyst dosage over $MAlPO_4$

Catalyst	Catalyst dosage(g)	Conversion (%)	Product selectivity (%)	
			CO	O_2
Mg-$AlPO_4$	0.5	99.3237	44.5147	55.4855
	1.5	24.1327	76.4858	23.5141
	2.5	23.1289	72.9442	27.0558
Mn-$AlPO_4$	0.5	74.0109	52.3016	47.6983
	1.5	13.3290	78.3547	21.6452
	2.5	22.9897	75.3485	24.6515

Time: 1 h, Temperature: 60 °C, Flow rate: 0.5 ml/min

Table 4. Effect of Time on stream over $MAlPO_4$

Catalyst	Time (h)	Conversion (%)	Product selectivity (%)	
			CO	O_2
Mg-$AlPO_4$	1	24.6846	91.2034	8.7966
	2	26.5441	74.7119	25.2881
	3	22.2317	38.0924	22.2317
	4	16.0788	58.5435	41.4565
	5	25.0261	61.8846	38.1953
Mn-$AlPO_4$	1	18.2146	83.7317	16.2682
	2	12.8382	77.9689	22.0311
	3	16.8197	92.7841	7.2159
	4	18.6417	85.9734	14.0373
	5	26.4486	88.2549	11.7450

Time: 1 h, Temperature: 60 ˚C, Flow rate: 0.5 ml/min

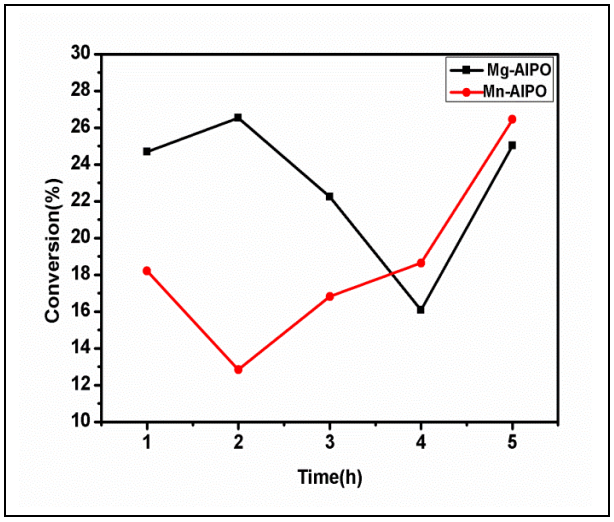

Fig. 11: Effect of Time on stream on the decomposition of CO_2 over $MAlPO_4$

5. CONCLUSION

Sol-gel method was used to make nanoporous Mg-$AlPO_4$ and Mn-$AlPO_4$, utilizing n-butyl amine as a new template. Powder X-ray Diffraction, Fourier Transform Infrared and Scanning Electron Microscope techniques were used to characterize the synthesized materials. The formation of $AlPO_4$ materials has been proved using these methods. A carbon dioxide decomposition reaction was used to investigate the catalysts' catalytic activity. Carbon dioxide was decomposed in a catalytic reactor using Mg-$AlPO_4$ and Mn-$AlPO_4$ as catalysts. Temperature, flow rate, catalyst dose and duration on stream were optimized in the lab for maximum CO_2 conversion. The molecules of carbon dioxide were broken down into carbon monoxide and oxygen and the decomposed products were analyzed by Gas Chromatography. The decomposition of carbon dioxide by the synthesized materials was very effective even at very low temperature (60 ˚C). Above 90% decomposition of carbon dioxide was observed over Mg-$AlPO_4$, whereas 70% decomposition of carbon dioxide was observed over Mn-$AlPO_4$ material, proving that Mg-$AlPO_4$ was relatively better than Mn-$AlPO_4$.

FUNDING

This research received no specific grant from any funding agency in the public, commercial, or not-for-profit sectors.

CONFLICTS OF INTEREST

The authors declare that there is no conflict of interest.

REFERENCES

Anastas, P. T., Kirchhoff, M. M. and Willia, T. C., Catalysis as a foundational pillar of green chemistry, *Applied Catalysis A-General*, 221(1-2), 03-13(2001). https://doi.org/10.1016/S0926-860X(01)00793-1

Campelo, J. M., Jaraba, M., Luna, D., Luque, R., Marinas, J. M. and Romero, A. A., Effect of phosphate precursor and organic additives on the structural and catalytic properties of Amorphous Mesoporous AlPO4 Materials, *Chem. Mater*., 15, 3352-3364(2003). https://doi.org/10.1021/cm030206+

Campelo, M., Marinas, J. M., Mendioroz, S. and Pajares, J. A., Texture and surface chemistry of aluminium phosphates, *J. Catal.*, 101(2), 484-495(1986). https://doi.org/10.1016/0021-9517(86)90275-7

Cheralathan, K. K., Kannan, C., Arabindoo, B., Palanichamy, M. and Murugesan, V., Ethylation of toluene over aluminophosphate molecular sieves in the vapour phase, *Ind. J. Chem. Tech.*, 39(9), 921-927(2000).

Gao, Q., Chen, J., Xu, R. and Yue, Y., Synthesis and characterization of a family of amine-intercatalated lamellar aluminophosphates from alcoholic system, *Chem. Mater*. 9(2), 457-462(1997). https://doi.org/10.1021/cm9602611

Hardie, S. M. L., Garnett, M., Fallick, A. E., Rowland, A. P., Carbon-dioxide capture using a zeolite molecular sieve sampling system for isotopic (13C and 14C) studies of respiration, *Radiocarbon*, 47, 441-451(2005). https://doi.org/10.1017/S0033822200035220

Liu, Y., Lotero, E. and Godwin, J. G., Jr., Effect of water on sulfuric acid-catalyzed esterification, *J. Mol. Catal. A-Chem.*, 245(1-2), 132-140(2006). https://doi.org/10.1016/j.molcata.2005.09.049

Pai, S. M., Newalkar, B. L. and Choudary, N. V., Microwave-hydrothermal synthesis and characterization of silico-aluminophosphate molecular sieve: SSZ-51, *Micropor. Mesopo. Mat*., 112, 357-367(2008). https://doi.org/10.1016/j.micromeso.2007.10.010

Ruthven, D. M., *Principle of adsorption & adsorption processes*, John Wiley & sons, (1984).

Smit, B. and Maesen, T. L. M., Towards a molecular understanding of shape selectivity, *Nature*, 451, 671-678(2008). https://doi.org/10.1038/nature06552

Taguchi, A. and Schuth, F., Ordered mesoporous materials in catalysis, *Microporous Mesoporous Mater.*, *77(1)*, 01-45(2005). https://doi.org/10.1016/j.micromeso.2004.06.030

Tanev, P. T., Pinnavaia, T. J., A neutral templating route to mesoporous molecular sieves, *Science*, 267(5199), 865-867(1995). https://doi.org/10.1126/science.267.5199.865